ELSEVIER

Carbohydrate Research 316 (1999) 14–25

CARBOHYDRATE RESEARCH

The relative ability of aldoses and deoxyaldoses to reduce Cr^{VI} and Cr^{V}. A comparative kinetic and mechanistic study

Sandra Signorella, Verónica Daier, Silvia García, Roxana Cargnello, Juan Carlos González, Marcela Rizzotto, Luis F. Sala *

Departamento de Química-Física, Facultad de Ciencias Bioquímicas y Farmacéuticas (UNR), Suipacha 531, 2000 Rosario, Argentina

Received 2 September 1998; revised 18 December 1998; accepted 5 January 1999

Abstract

Oxidation of the aldoses (Ald) D-glucose, D-allose, D-mannose, D-galactose, 6-deoxy-D-galactose (D-fucose) and 2,6-dideoxy-D-*ribo*-hexose (digitoxose) by Cr^{VI} yields the aldonic acid and Cr^{3+} as final products when an excess of sugar over Cr^{VI} is used. The redox reaction occurs through $Cr^{VI} \rightarrow Cr^{III}$ and $Cr^{VI} \rightarrow Cr^{V} \rightarrow Cr^{III}$ paths. The rate laws for the Cr^{VI} and Cr^{V} oxidation reactions are expressed by: $-d[Cr^{VI}]/dt = k_H[Ald][Cr^{VI}]$ and $-d[Cr^{V}]/dt = k_b K_b[Ald][Cr^{V}]/(1 + K_b[Ald])$, where k_H, k_b and K_b are the kinetic parameters independent of the [Ald] and [oxidant], and the relative aldoses reactivity with both Cr^{VI} and Cr^{V} is 2,6-dideoxy-D-*ribo*-hexose > D-galactose > D-allose > D-glucose ≈ 6-deoxy-D-galactose, at 33 °C. Intermediate sugar alkoxide radicals could be trapped with 5,5-demethyl-1-pyrroline *N*-oxide (DMPO) and observed by electron paramagnetic resonance (EPR) as a multiline signal at $g = 2.003$. Cr^{V} is formed in a rapid step by the reaction of the sugar$^{\bullet}$ radical with Cr^{VI}. The substrate is oxidised at a comparable rate by Cr^{VI} and Cr^{V}, especially at higher [Ald], and the reduction of Cr^{VI} occurs concurrently with Cr^{V}. The EPR spectra show that five- and six-coordinate oxochromate(V) intermediates are formed, with the aldose and/or the aldonic acid acting as bidentate ligands. Penta-coordinate Cr^{V} species are present at any $[H^+]$, whereas hexa-coordinate ones require stronger acid conditions.

Keywords: Kinetics mechanism; Chromium; Aldohexoses; Redox intermediates

1. Introduction

Cr^{VI} is a potential hazard both in a biological and an ecological context [1]. The observation of Cr^{V} and Cr^{IV} intermediates in the selective oxidation of organic substrates by Cr^{VI} and their implication in the mechanism of Cr-induced cancers [2–6] has generated a considerable amount of interest in their chemistry and biochemistry [7–11]. The biological reduction of Cr^{VI} to lower states has been observed with a wide variety of naturally occurring cellular reductants [12–14]. Ligands that possess two vicinal oxygen atoms are able to form five-membered rings about the metal ion, such as 1,2-diols and α-hydroxy acids, are effective as non-enzymatic reductants and complexation agents towards hypervalent chromium, and can stabilise the labile oxidation states of chromium [15–19]. For this reason, it is interesting to study the ability of monosaccharides to reduce Cr^{VI} to Cr^{III}, a

* Corresponding author. Fax: +54-341-4350-214.
E-mail address: inquibir@satlink.com (L.F. Sala)

0008-6215/99/$ - see front matter
PII: S0008-6215(99)00012-9

relevant aspect of the transport of metal ions through soils causing environmental pollution.

We are studying the possible fate of Cr^{VI} and Cr^{V} in biological systems by examining reactions of Cr^{VI} with low-molecular-weight molecules [20–29].

In previous work we have studied the reaction between Cr^{VI} and certain aldoses (mannose, ribose) [20,30] and deoxyaldoses [20,23,25,30] (2-deoxy-D-*arabino*-hexose, 2-deoxy-D-*erythro*-pentose, rhamnose). These studies provided the first information about the relative abilities of these monosaccharides to reduce chromate. Comparing these aldoses with the 2-deoxy derivatives, we found that the lack of the 2-OH group accelerates the total reaction and that the 6-OH group could bind Cr^{VI} in an intermediate ester. However, a larger number of sugars has to be examined in order to know if these finding can be generalised. In most of the studies performed previously [31–33], no mechanistic proposals were presented and the kinetic parameters were referred to the global redox reaction, without discrimination of the sugar oxidation by Cr^{VI} and Cr^{V}, a very important fact especially when the Cr^{VI} and Cr^{V} oxidation rate constants are of the same order of magnitude [34].

This work is aimed at analysing the factors influencing the rate of oxidation of several monosaccharides by Cr^{VI} and by the intermediate Cr^{V} formed during the reaction course. All of the redox reactions described in this work were performed under the same set of experimental conditions and the reactivities of the different sugars are compared and differences interpreted in terms of the ability of the sugars to bind Cr^{VI}/Cr^{V}.

2. Results and discussion

Rate studies.—In the chromic oxidation of D-galactose (Gal), D-allose (All), D-glucose (Glc) and 6-deoxy-D-galactose (6dGal) the absorbance versus time curves at 350 nm exhibit a monotonic decrease of absorbance that cannot be described by a single exponential decay.

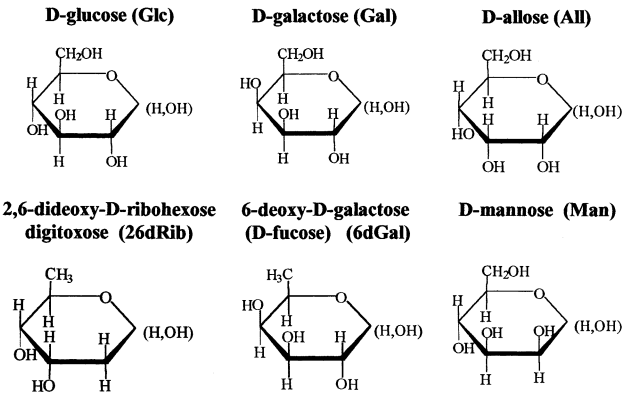

At this wavelength, kinetic traces show an initial deviation from first-order decay over short time periods, which could be adequately described by the set of consecutive first-order reactions of Scheme 1.

It is known that Cr^{V} species absorb strongly at 350 nm and may superimpose Cr^{VI} absorbance [34]. Thus, assuming the Cr^{VI} and Cr^{V} absorption superimposition, the absorbance at 350 nm, at any time during the reaction, is given by

$$Abs^{350} = \varepsilon^{VI}[Cr^{VI}] = \varepsilon^{V}[Cr^{V}] \quad (1)$$

Combining Eq. (1) with rate expressions [35] derived from Scheme 1 yields:

$$Abs^{350} = Abs_0 \exp(-k_6 t) + k_6 \varepsilon^{V}[Cr^{VI}]_0 \times \{\exp(-k_5 t) - \exp(-2k_6 t)\} \times (2k_6 - k_5)^{-1} \quad (2)$$

In this equation, ε^{V} refers to the molar absorptivity of Cr^{V} at 350 nm and was assumed to be the same as for the complex $[Cr^{V}(O)(ehba)_2]^-$ [36]. Parameters k_6 and k_5 refer to the rate of disappearance of Cr^{VI} and Cr^{V}, respectively, and were evaluated from a non-linear iterative computer fit of Eq. (2). The calculated kinetic parameters, k_6 and k_5, for various concentrations of the studied aldoses in 0.75 M $HClO_4$, are summarised in Table 1. In multiple measurements, the reproducibility of the two rate constants is better than 10%. Values of k_6 and k_5 were confirmed

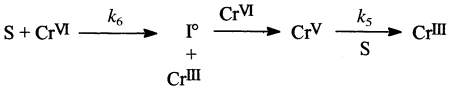

Scheme 1. S, Organic substrate; I°, intermediate radical.

Table 1
Observed first-order rate constants k_5 and k_6 (s^{-1}) for different concentrations of monosaccharides[a]

[Sugar] (M)	6dGal		Glc		All		Gal	
	$10^4\ k_6$	$10^4\ k_5$	$10^4\ k_6$	$10^4\ k_5$	$10^4\ k_6$	$10^4\ k_5$	$10^4\ k_6$	$10^4\ k_5$
0.02							2.3(1)	9.0(1)
0.04	1.00(6)	3.74(4)	1.7(2)	3.6(4)	2.9(1)	5.5(8)	4.9(1)	12.5(6)
0.06							7.5(1)	18(1)
0.08	2.35(1)	4.74(9)	3.1(2)	5.2(8)	5.7(3)	13(1)	9.7(1)	22(1)
0.10							12(1)	23(1)
0.12	3.12(1)	6.7(2)	4.4(1)	6.6(2)	8.7(2)	17(1)		
0.14							17(1)	28(1)
0.16	3.8(1)	9.2(4)	5.7(1)	8.9(2)	11(1)	18(1)	19(1)	28(1)
0.20	5.17(9)	9.6(4)	7.3(6)	9.6(9)	15(1)	21(2)		

[a] $I = 1$ M; $T = 33$ °C; $[H^+] = 0.75$ M; $[Cr^{VI}]_0 = 8 \times 10^{-4}$ M.

from the experimental absorbance data at 570 nm. At this wavelength the Cr^{III} formation can be followed and changes in Cr^{III} absorbance can be described by Eq. (3):

$$\mathrm{Abs}^{570} = \mathrm{Abs}_{\infty}^{570} + \mathrm{Abs}_{\infty}^{570}\{(k_5 - k_6)\exp(-2k_6t) - k_6\exp(-k_5t)\}/(2k_6 - k_5) \quad (3)$$

Values of k_6 and k_5 calculated by Eq. (3) coincide with those obtained by using Eq. (2).

2,6-Dideoxy-D-*ribo*-hexose (26dRib) behaves in a rather different way. The variation of the absorbance at 350 nm can be described by a single exponential decay from which k_{obs} ($2k_6$) could be determined (Table 2). In this case, $k_5 \gg k_6$, and Cr^V does not interfere the absorbance due to Cr^{VI}. This assumption was confirmed by the fit of the absorbance data at 570 nm to Eq. (4),

$$\mathrm{Abs}^{570} = \mathrm{Abs}_{\infty}^{570}\{1 - \exp(-k_{obs}t)\} \quad (4)$$

and is consistent with the observation of an isosbestic point at 525 nm under conditions employed to follow Cr^{III} at 570 nm.

Cr^{VI} oxidation of monosaccharides.—For all the sugars under study, in 0.75 M $HClO_4$, plots of $2k_6$ versus [aldose] ([Ald]) gave good straight lines from which values of k_h were determined (Table 3). The rate law is then expressed by

$$-\mathrm{d}[Cr^{VI}]/\mathrm{d}t = 2k_6[Cr^{VI}]_T = k_h[Ald][Cr^{VI}]_T \quad (5)$$

where $[Cr^{VI}]_T$ represents the total Cr^{VI} concentration.

A mechanism taking account of the substrate first-order dependence and the selective oxidation of the aldose to the aldonic acid (Alda[1]) (the only detected reaction product when the sugar/Cr^{VI} is ≥ 25), is proposed in Scheme 2.

In acid medium, Cr^{VI} exists mainly as $HCrO_4^-$ [37]. Thus, the first step of the mechanism proposed in Scheme 2 may be interpreted as the formation of a monochelate with the aldose acting as a bidentate ligand bound to Cr^{VI} at O-1 and O-2 to yield the anionic species A^-. Even when several linkage isomers might be formed by coordination of the sugar with Cr^{VI} via any properly disposed hydroxyl groups, we propose a complex with

Table 2
Observed first-order rate constants (k_{obs}) for 26Rib at different concentrations of $HClO_4$[a]

[26dRib] (M)	$10^4\ k_{obs}$ ($2k_6$) (s^{-1}) at $[HClO_4]$ (M)			
	0.25	0.50	0.60	0.75
0.02	3.21(4)	10.8(2)	14.7(3)	21.8(3)
0.04	6.01(3)	20.8(5)	26.7(2)	40.7(7)
0.06	10.1(1)	35.5(5)	46.2(5)	67.4(8)
0.068	10.5(3)	35.8(4)	48(2)	70(2)
$10^2\ k_h$ ($M^{-1}\ s^{-1}$)	1.6(3)	5.1(2)	6.9(2)	10.1(3)

[a] $I = 1$ M; $T = 33$ °C; $[Cr^{VI}]_0 = 8 \times 10^{-4}$ M.

[1] The term Alda is used here to denote aldonic acid, and to differentiate it from AldA, which would imply alduronic acid.

Table 3
Calculated second-order (k_h and k_b) and Cr^V (K_b) formation rate constants

	6dGal	Glc	All	Gal
$10^3\ k_h$ ($M^{-1}\ s^{-1}$)	2.6(4)	3.7(6)	7.2(1)	12(1)
$10^3\ k_b$ ($M^{-1}\ s^{-1}$)	2.2(7)	2.0(4)	4.2(9)	4.6(4)
K_b	4(2)	5(1)	5(2)	11(2)

the anomeric hydroxyl group bound to Cr^{VI} because it should be the precursor of the slow redox steps—the oxidation of the aldose occurs at this position. This intermediate then yields the redox product through the slow step. The k_h in the rate law corresponds to kK in this mechanism. This means that the relative reactivity of the sugars may be interpreted by comparing the rate of decomposition of the Cr^{VI} ester; i.e., the higher reactivity should reflect the faster decomposition of the intermediate complex and, consequently, the easier electron transfer within a less-stable species.

For 26dRib, the dependence of k_h on the $[H^+]$ was examined. A plot of k_h (Table 2) versus $[H^+]^2$ gave a straight line with a positive intercept, showing that the second-order rate constant may be expressed as consisting of an acidity-independent and an acidity-dependent term:

$$k_h = k_0 + k_1[H^+]^2 \quad (6)$$

where $k_0 = 6.7(2) \times 10^{-3}\ M^{-1}\ s^{-1}$ and $k_1 = 1.6(1) \times 10^{-1}\ M^{-3}\ s^{-1}$.

The two terms in the rate law (Eq. (6)) result from the fact that there are at least two transition states, differing in composition but similar in energy, through which the reduction of Cr^{VI} can proceed. Thus, the oxidation of 26dRib by Cr^{VI} should occur through two parallel slow steps leading to the redox products.

The first step of the mechanism proposed for the oxidation of 26dRib in Scheme 3 corresponds to the formation of a 1:1 26dRib–Cr^{VI} binary complex, with 26dRib acting as a monodentate ligand bound to Cr^{VI} at the anomeric hydroxyl group to yield the anionic

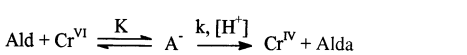

Scheme 2. $A^- = [(AldH_{-2})CrO_2(H_2O)OH]^-$.

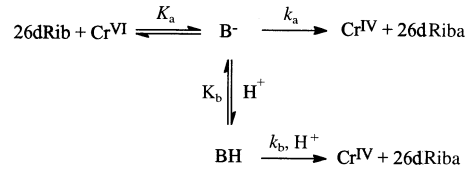

Scheme 3. $B^- = [(26dRibH_{-1})CrO_2(H_2O)(OH)_2]^-$.

species B^-. This intermediate may decompose directly to the products or give BH. This monoprotonated intermediate yields the redox products through an acid catalysed step.

For any of the studied sugars, after the slow steps, reactions (7)–(9) may take place:

$$Sugar + Cr^{IV} \rightarrow Sugar^{\bullet} + Cr^{III} \quad (7)$$

$$Sugar^{\bullet} + Cr^{VI} \underset{slow}{\rightarrow} Sugar\ acid + Cr^{V} \quad (8)$$

$$Sugar + Cr^{V} \rightarrow Sugar\ acid + Cr^{III} \quad (9)$$

Cr^{IV} formed in the slow steps yields the final Cr^{III} and the sugar radical in a subsequent fast step. The formation of these sugar radicals is supported by the observed polymerisation after addition of acrylonitrile. In addition, a spin trap was used to detect any sugar radical intermediate formed during the reduction of Cr^{VI} by the monosaccharide. In any case, the addition of the spin trap 5,5-dimethyl-1-pyrroline *N*-oxide (DMPO) to the reaction mixture resulted in the appearance of a spin adduct signal at $g = 2.003$ (Fig. 1) with splitting constants of $a_N = 7.48 \times 10^{-4}\ cm^{-1}$, $a_H = 3.65 \times 10^{-4}\ cm^{-1}$ ($\times 2$). The observation of the signal corresponding to a DMPO/sugar radical adduct confirms our proposal. Cr^V forms by rapid reaction of the radical and Cr^{VI}, and it can further oxidise the sugar to yield the final redox products, as discussed next.

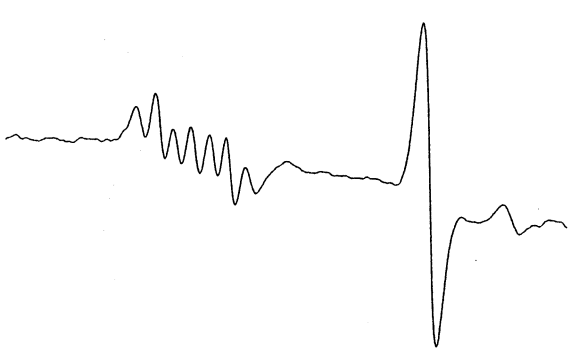

Fig. 1. X-band EPR spectrum recorded on a 0.1 M $HClO_4$ solution containing 0.0375 M Cr^{VI}, 0.375 M Ald and 0.09 M DMPO, recorded 4 min after mixing. $T = 25$ °C, modulation amplitude: 0.514 G, centre field: 3450 G.

Cr^V oxidation of the sugars.—In 0.75 M $HClO_4$, the effect of the [Ald] on k_5 can be written as

$$k_5 = k_b K_b[\text{Ald}]/(1 + K_b[\text{Ald}]) \quad (10)$$

Plots of k_5 versus [Ald] (Ald = Gal, All, Glc, 6dGal) show kinetic profiles yielding saturation curves [20,24] from which values of k_b and K_b were determined (Table 3). The saturation curves reveal that the intermediate Cr^V complex is formed faster and remains longer than the corresponding intermediate Cr^{VI} ester. A mechanism taking into account these kinetic results together with the structural evidences will be discussed in the next section.

Structure of intermediate sugar–Cr^V complexes.—The reaction of Cr^{VI} with an excess of 2–100 times of the monosaccharide, in the pH 3–7 range, at 25 °C, generates an EPR spectrum dominated by a single detectable signal at $g_{iso} \cong 1.979$ with the four weak ^{53}Cr (9.55% abundance, $I = 3/2$) hyperfine peaks at $16.4(3) \times 10^{-4}$ cm^{-1} spacing, typical of five-coordinate oxochromate(V) complexes [38–40]. In this pH range, Cr^V remains in solution several days. We found that by varying the modulation amplitude, the superhyperfine (shf) pattern partially resolved [as shown for Glc–Cr^V in Fig. 2(a) and (b)], and the Cr^V EPR spectrum resulted in a composite of several Cr^V species. The proton shf coupling, together with the g_{iso} and A_{iso} values, have been shown to be useful in determining the binding of 1,2-diolate moieties of sugars to the Cr^V centre [20,40], where 1,2-diolate moiety refers to any pair of properly disposed vicinal hydroxyl groups. However, if a molecule has more than one pair of such hydroxyl groups, the g_{iso} and shf splitting values are essentially the same for the several Cr^V–sugar complexes formed via any of these vicinal hydroxyl groups, but they differ from complexes formed with the sugar acting as a mono- or tridentate (through a triolate moiety) ligand bound to Cr^V.

The g_{iso} values for all of the Ald–Cr^V EPR signals (Table 4) are in the range of those expected for five-coordinate oxochromate(V) complexes, and the relative proportion of each species in the reaction mixture depends on the reaction extent and not on the proton concentration or the saccharide:Cr^{VI} ratio. This can be observed in Fig. 2(b) and (c) for Glc–Cr^V. Thus, the relative intensity of the peaks varies with time, and, for any pH, there is always a moment in which the spectra may superimpose each other.

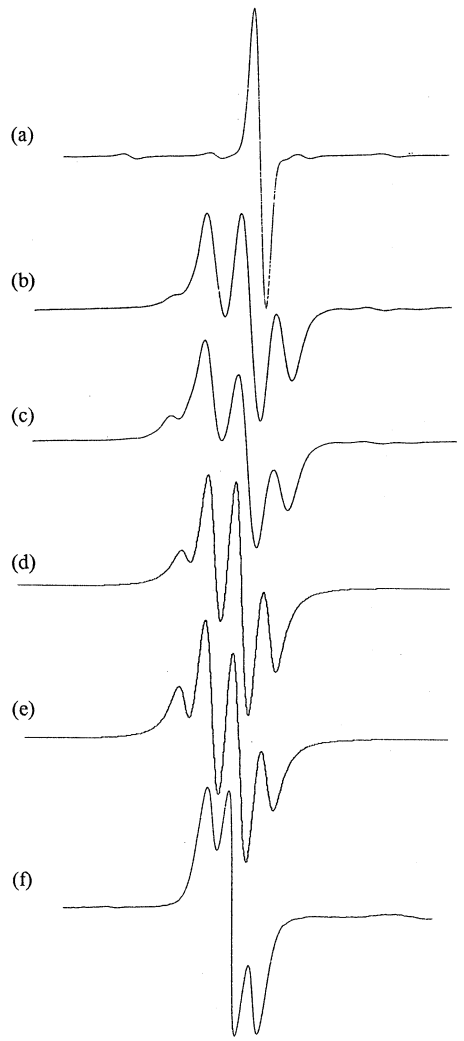

Fig. 2. X-band EPR spectra of a Glc–Cr^{VI} reaction mixture at pH 5: (a) 5 min after mixing, modulation amplitude = 0.4; (b) 5 min after mixing, modulation amplitude = 0.056; (c) 1 day after mixing, modulation amplitude = 0.056; and the simulated spectra for (d) $g_1/g_2 = 1.2$ and (e) $g_1/g_2 = 0.3$; (f) X-band EPR spectrum of a 26dRib–Cr^{VI} reaction mixture, 5 min after mixing at pH 7. $T = 25$ °C.

The composition of the Cr^V species in solution may be estimated from the isotropic EPR parameters based on the empirical method developed by Lay and co-workers [41] together with the shf pattern. Based on this criterion, an estimation of the Cr^V species present in the mixture was made. For the Glc–Cr^V system, in the pH 3–7 range, at 25 °C, the EPR spectrum was found to be composed (signals were decon-

Table 4
Cr^V EPR spectral parameters

Sugar	pH	g (m)[a]	10^4 a_H (cm^{-1})
Glc	3–7	1.9793 (q)	0.94
		1.9789 (t)	0.92
Man	3	1.9791 (t)	0.92
		1.9795 (q)	0.93
	5–7	1.9791 (t)	0.92
26dRib	3	1.9789 (t)	0.92
		1.9794 (q)	0.93
	7	1.9789 (t)	0.92
Gal	3	1.9789 (q)	0.92
		1.9796 (quint)	0.93
	5–7	1.9789 (q)	0.92
		1.9785 (quint)	0.94
6dGal	3–7	1.9785 (t)	0.92
		1.9786 (quint)	1.19
		1.9794 (t)	0.92
All	3–7	1.9785 (t)	0.92
		1.9787 (quint)	1.19
		1.9794 (t)	0.92

[a] t, Triplet; q, quartet; quint, quintet.

voluted by fitting the spectra by Lorentzian derivatives) of two Cr^V species at $g_1 = 1.9789$ and $g_2 = 1.9793$. The best fit of the spectrum yields the spectral parameters summarised in Table 4. The g_{iso} values obtained for the two signals are those expected for five-coordinate oxochromate(V) complexes [41]; while the different shf patterns indicate the number of carbinolic protons coupled to the Cr^V centre in each case. The shf splitting of the signal at g_1 arises from the coupling of two equivalent protons and may be attributed to a Cr^V complex with one Glc molecule acting as a bidentate ligand at a 1,2-diolate moiety. This coordination mode can occur in a number of ways, however, the complex with the anomeric hydroxyl group bound to Cr^V should be the only redox active intermediate—the oxidation of the aldose occurs only at this position—in rapid equilibrium with any other linkage isomer giving rise to this signal. The shf splitting of the signal at g_2 may be assumed to arise from two different binding modes of the two ligand molecules, Glc and Glca, coordinated to Cr^V via a 1,2-diolate (Glc) and the α-hydroxocarboxylate (Glca) donor sites, respectively. Variation of the relative intensity of the EPR lines may be rationalised as a consequence of the variation of the relative g_1:g_2 ratio. In Fig. 2, the simulated spectra correspond to 6:5 (d) and 3:10 (e) g_1:g_2 ratios. One quartet and one triplet were also observed for Man and 26dRib at pH 3 (Table 4), whereas at higher pH (5–7) only the triplet is observed (Fig. 2(f)). A mechanism taking into account the structural evidence for the Cr^V intermediate complexes together with the kinetics results, previously discussed, is given in Scheme 4.

Such as proposed in Eq. (8), Cr^V is formed by reaction of the sugar radical (detected by EPR) and Cr^{VI}. Besides, from the kinetic data, we know that the Cr^V intermediates form before the redox reaction occurs. Thus, in the scheme, the intramolecular electron transfer process takes place within complexes I and II and the formation of these complexes requires an additional Ald molecule, such as deduced from the kinetic data obtained from the spectrophotometric measurements (Eq. (10)). Besides, for Man and 26dRib, at pH > 5, the redox path takes place within a complex of type II only. For 26dRib, the formation of the Cr^V complex of type I implies 26dRiba acting as a bidentate ligand through the β-hydroxy acid moiety, which yields a 6-membered ring in the intermediate complex. Since Cr^V prefers to form 5-membered ring chelates [42], the formation of this 6-membered ring chelate should probably be responsible for the $k_5 \gg 2k_6$ relative values observed for the oxidation of this sugar in acidic medium.

For the Gal–Cr^{VI} system, in the pH 3–7 range, the spectra are dominated by a quartet

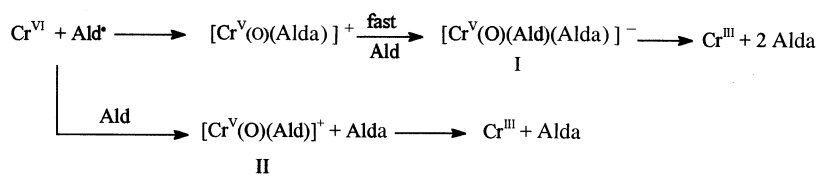

Scheme 4. Ald: Glc, D-mannose (Man), 26dRib; Alda (aldonic acid): Glca, Mana, 26dRiba.

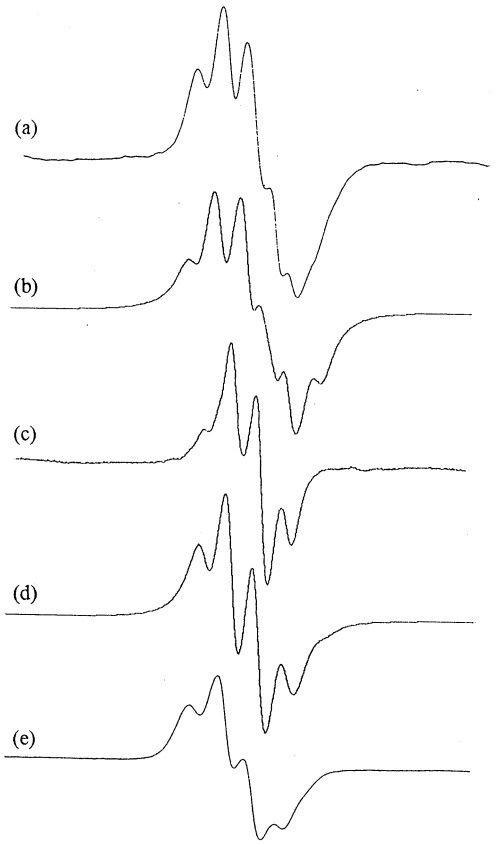

Fig. 3. X-band EPR spectra of a Gal–Cr^{VI} reaction mixture (a) 5 min after mixing at pH 3; (b) 1 day after mixing at pH 5; (c) at pH 7; (d) the simulated spectrum for $g_1/g_2 = 5$; (e) X-band EPR spectrum of a 6dGal–Cr^{VI} reaction mixture, 5 min after mixing. $T = 25$ °C.

at 1.9789 (Table 4). The g_{iso} and shf pattern clearly indicate that CrO^{3+} coordinates two ligand molecules, one Gal and one Gala, acting through a 1,2-diolate and the α-hydroxocarboxylate donor sites. In the pH 5–7 range, the minor signal ($g_{iso} = 1.9785$) can be attributed to the isomer with Gal and Gala binding Cr^V via a 1,2-diolate moiety while at pH 3 the quintet ($g_{iso} = 1.9796$) may be assigned to the $[Cr^V(O)(Gal)_2]^-$. Fig. 3(a) and (b) shows the spectra of a reaction mixture at pH 3 at two different reaction times and Fig. 3(c) and (d) corresponds to a reaction mixture at pH 7 with the simulated spectrum. A summary of the species involved in the Gal–Cr^V system is shown in Scheme 5.

Finally, 6dGal and All behave similarly and form with Cr^V three intermediate complexes characterised by two triplet and one quintet in the EPR spectrum, in the pH 3–7 range [Table 4, Fig. 3(e)]. The Cr^V complexes formed in this case may be rationalised as shown in Scheme 6 with the aldose acting through the 1,2-diolate moiety in the five-coordinate oxochromate(V) mono- (I and V) and bis-chelate (III).

At $[HClO_4] \geq 0.1$ M, the reaction of Cr^{VI} with excess Ald resulted in the formation of three or four types of relatively long-lived Cr^V species. The relative intensity of the Cr^V EPR signals depends on the $[H^+]$ (Fig. 4), but is independent of the Ald:Cr^{VI} ratio employed (from 2:1 to 100:1). The g_2, g_3 and g_4 values are significantly lower than the values observed for the five-coordinate oxochromate(V) complexes and, since the g values of the Cr^V species are very sensitive to coordination [41], they may be assigned to six-coordinate oxochromate(V) complexes [39]. However, the lack of a resolved shf pattern from the protons under these acid conditions, prevented a more detailed analysis of this signals. Table 5 shows that for $[H^+] = 0.1$ M, the five-coordinate species (g_1) is the major one, but at higher $[H^+]$ one of the six-coordinate species (g_3) becomes the major one. Thus, the five-coordinate oxochromate(V) complexes are formed at any $[H^+]$, whereas the formation of the six-coordinate species requires acid conditions. All the three or four signals decay at essentially the same rate, meaning that the relative intensities observed in the spectra and detailed in Table 5 are only dependent on the proton concentration and do not depend on the reaction time, i.e., the time course of the peak-to-peak height of the first derivative of the EPR signals as a function of time for an initial ratio 6dGal:$Cr^{VI} = 10:1$, at $[H^+] = 0.15$ M, revealed that the three signals decay at comparable rates with $k_5 = 1.2 \times 10^{-4}$ s^{-1}. In this way we can express that the hexa- to penta-coordinated species ratio is a function of the $[H^+]$ but it remains constant during the reaction course, when an excess of hydrogen ions over Cr^{VI} is present in the reaction mixture. In other words, these Cr^V intermediates are in rapid equilibrium compared with the time scale of their subsequent reduction to Cr^{III}. These rates increased with decreasing pH, indicating that proton catalysis is present. A similar behaviour had been previously observed for the reaction of 2-deoxy-D-glucose (2dGlc) and 2-deoxy-D-ribose (2dRib) with Cr^{VI} [23,25,30].

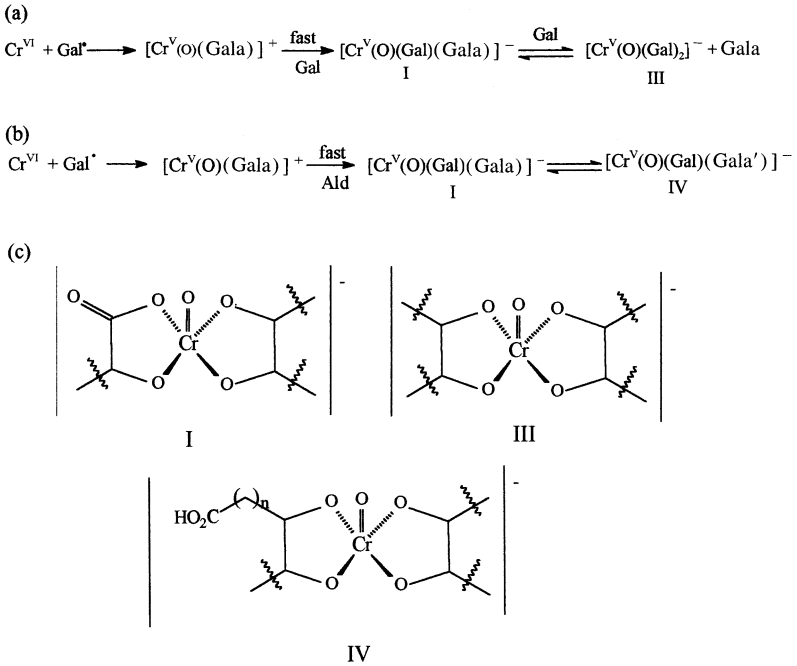

Scheme 5. At any pH, I (III or IV) yields Cr^{III} and Gala as final products. (a) pH 3; (b) pH 5–7; (c) coordination modes for Gal and Gala in complexes I, III and IV.

At any $[H^+]$, the ultimate fate of the chromium in these reactions is a Cr^{III} species and a typical broad Cr^{III} EPR signal centred at $g \sim 1.98$ is always observed at later time points.

Conclusions.—For all these aldoses, the 1-OH hemiacetalic function reacts faster than the primary or any of the secondary alcoholic groups. The aldonic acid (or/and the corresponding lactone) as the only reaction product easily proves this. As a consequence, the intramolecular electron-transfer should occur within a five-membered chelate chromate (the five-membered chromate esters are the most favourably formed [42]) with the 1-OH group as one of the coordination sites.

The sugars studied, except the 26dRib, are oxidised at comparable rates by Cr^{VI} and Cr^{V}, especially at higher [Ald]. These results show that the reduction of Cr^{VI} occurs concurrently with Cr^{V}, and consequently Cr^{V} and Cr^{VI} absorbances at 350 nm are always superimposed, and this fact has to be taken into account. The tendency in the reactivity of these aldoses: 26dRib > Gal > Man [43] > All > Glc ≈ 6dGal reveals that the axial 4-OH in the Gal stereoisomer has the highest rate accelerating effect, followed by the axial 2-OH in Man and 3-OH in All; finally, Glc, with all the ring substituents in pseudo-equatorial position, is oxidised slower than the other aldohexoses. In the case of 26dRib the absence of the 2- and 6-OH chelation sites accelerates the reaction rate, as observed (though, in a lower extent) for 2dGlc and 2dRib, when compared with Glc and Rib, respectively [25,30]. This effect is attributed to the higher stability of the five-membered chelation ring versus the mono-coordinated ligand [42]. In other words, the monosaccharide that forms the less 'stable' aldose–Cr^{VI} chelate with the structure required for the intramolecular hydride transfer will be that with the higher redox rate. However, the absence of the 6-OH in 6dGal does not act as an accelerating factor, but on the contrary, the reaction occurs at the slowest rate. A suitable explanation should probably be a different conformation of the aldose in the intermediate complex, such as that proposed in Fig. 5.

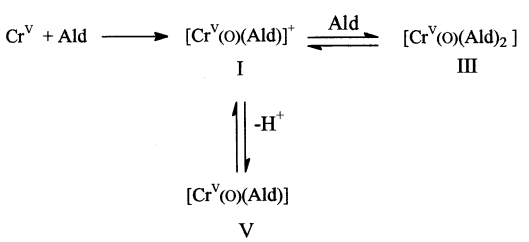

Scheme 6. Ald: 6dGal, All.

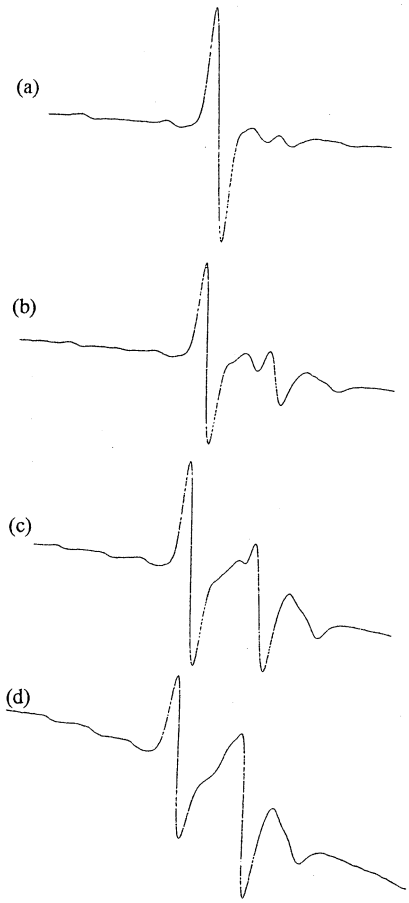

Fig. 4. X-band EPR spectra of a Gal–Cr^{VI} reaction mixture, 5 min after mixing at $[H^+]$ (a) 0.1 M; (b) 0.25 M; (c) 0.5 M; (d) 0.75 M. $T = 25$ °C.

Sugars stabilise Cr^V yielding penta- and hexa-coordinate oxochromate(V) complexes depending on the $[H^+]$. In any case, the relative reactivity of the monosaccharides towards Cr^V is the same as observed towards Cr^{VI}. This behaviour should reflect the similar nature of the intermediate chromate complexes formed between the aldoses and Cr^{VI}/Cr^V. At $[H^+] > 0.1$ M, penta- and hexa-coordinated complexes form; these complexes are in rapid equilibrium and react at the same rate yielding intramolecular redox reactions rapidly. At pH > 2, only penta-coordinated Cr^V species form, indicating that the hexa-coordinate species formation requires acid catalysis. These two or three penta-coordinate Cr^V species form and decay at different rates. In this pH range, intramolecular redox reactions are very slow and Cr^V complexes remain in solution several days to weeks. The Cr^{III} formed as the ultimate fate of the chromium in these reactions corresponds to $Cr(H_2O)_6^{3+}$.

3. Experimental

Materials.—D-Glucose (Glc) (P.A., E. Merck), D-allose (All) (P.A., Fluka), D-mannose (Man) (Sigma grade), D-galactose (Gal) (Sigma grade), 6-deoxy-D-galactose (6dGal) (P.A., Fluka), 2,6-dideoxy-D-*ribo*-hexose (26dRib) (P.A., Fluka), potassium dichromate (Cicarelli c.a.), sodium perchlorate (Fluka grade), acrylonitrile (Aldrich grade) and

Table 5
Relative intensities of Cr^V EPR signals recorded 5 min after mixing the reactants, at different $[H^+]$

Sugar	g_1	g_2	g_3	g_4
Glc	1.9791	1.9742		1.9665
$[H^+]$				
0.10	4.3	1.0		0.2
0.25	1.4	1.0		0.2
0.50	1.0	1.0		0.2
0.75	0.8	1.0		0.2
Man	1.9791	1.9740	1.9713	1.9660
$[H^+]$				
0.10	9.8	1.7	1.0	
0.25	1.9	0.3	1.0	
0.50	0.7	0.1	1.0	0.06
0.75	0.4	0.03	1.0	0.04
26dRib	1.9792	1.9738	1.9707	
$[H^+]$				
0.10	5.9	1.6	1.0	
0.25	1.4	0.6	1.0	
0.50	0.6	0.3	1.0	
Gal	1.9789	1.9740	1.9709	1.9655
$[H^+]$				
0.10	23	1.4	1.0	
0.25	3.3	0.3	1.0	0.15
0.50	1.6	0.05	1.0	0.2
0.75	1.0		1.0	0.2
6dGal	1.9791	1.9740	1.9712	
$[H^+]$				
0.10	11	1.0	1.0	
0.25	3.0	0.5	1.0	
0.50	1.7	0.09	1.0	
0.75	0.8	0.06	1.0	
All	1.9791	1.9744	1.9714	
$[H^+]$				
0.10	7.30	0.63	1.0	
0.25	1.77	0.17	1.0	
0.50	0.98	0.12	1.0	

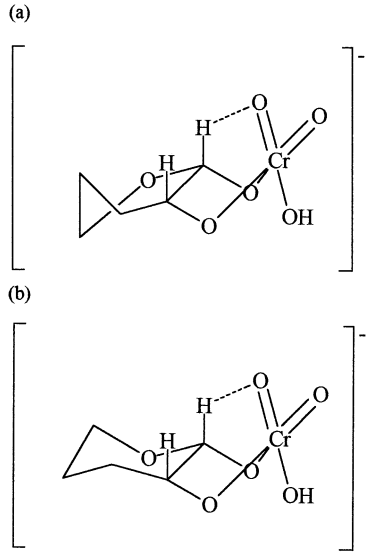

Fig. 5. Intermediate chromate chelate with two different conformations of the sugar ring.

perchloric acid (P.A., E. Merck) were used without further purification. Water was purified by deionisation followed by double distillation from a potassium permanganate solution.

For experiments performed in the pH 2–7 range, the pH of the solutions was adjusted by addition of 0.5 M NaOH and 0.5 M $HClO_4$.

The spin trap 5,5-dimethyl-1-pyrroline *N*-oxide (DMPO) (Aldrich grade) was purified by charcoal decolorisation. The method consists of successively treating the DMPO with activated charcoal until all free radical impurities disappeared by EPR spectroscopy [44].

Spectrophotometric measurements.—Most kinetics measurements were made at 350 nm, by monitoring the absorbance changes on a Guilford Response II spectrophotometer with fully thermostated cell compartments. Mixtures of $NaClO_4$ and $HClO_4$ were used to maintain a constant ionic strength (I) of 1.0 M. Reactant solutions were previously thermostated and transferred into a cell of 1 cm path length immediately after mixing, and the disappearance of Cr^{VI} was followed until at least 80% conversion. Experiments were performed at 33 °C unless otherwise mentioned. In most experiments the concentration of Cr^{VI} was kept constant at 8×10^{-4} M, while the sugar concentration was varied from 0.02 to 0.2 M. The first-order dependence of the rate upon $[Cr^{VI}]$ was verified for all sugars studied. The first-order rate constants were calculated at various $[Cr^{VI}]_0$, but at constant temperature, $[Ald]_0$, $[H^+]$ and I. As expected on the basis of a $-d(\ln[Cr^{VI}])/dt = k_{obs}$ rate law where $k_{obs} = f([Ald][H^+])$, k_{obs} was found to be essentially constant with increasing $[Cr^{VI}]_0$.

The formation of Cr^{III} was monitored at 570 nm ($[Cr^{VI}]_0 = 1.8 \times 10^{-2}$ M) and ratios of Ald:Cr^{VI} from 10:1 to 20:1, in 0.75 M $HClO_4$. At the end of the reaction the two d–d bands ascribed to Cr^{III} were observed at $\lambda_{max} = 410$ nm ($\varepsilon = 21$ dm^3 mol^{-1} cm^{-1}) and 571 nm ($\varepsilon = 17.5$ dm^3 mol^{-1} cm^{-1}). Both visible and UV spectral maxima and intensities are in close agreement with those observed for the $[Cr(H_2O)_6]^{3+}$ ion.

Product analysis.—Under the conditions used in the kinetic measurements (ratios of aldose (Ald) to Cr^{VI} from 25:1 to 250:1), qualitative identification of D-aldonic acid (Alda) as the reaction product was carried out by paper chromatography. Aldonic acids were identified against authentic samples using *n*-butanol/acetic acid/water (4:1:5 and 4:2:3) as eluent. Paper chromatograms were visualised by two kinds of development reagents: a three-stage dip of $AgNO_3$, NaOH and sodium thiosulphate and *p*-anisidine reagent [45,46].

Identification of the aldonic acid as the only reaction product was also made by ^{13}C NMR. In a typical experiment, a mixture of Ald (5.55 mmol) and $K_2Cr_2O_7$ (0.94 mmol) in 1.2 M $HClO_4$ (2 cm^3) was allowed to react at 33 °C. After the reaction had proceeded to completion, the mixture was stirred with a Dowex 50W-X8 cation exchange resin until all the Cr^{III} was removed from the solution and a concentrated sample was analysed by ^{13}C NMR. In each case, Alda (and/or the corresponding aldonolactone) and unreacted Ald were identified by comparison against authentic samples. For sugar to Cr^{VI} ratios < 10, formic acid and the lower aldonic acid were also observed by this technique. However, for the sugar to Cr^{VI} ratios used in the kinetic studies (sugar/$Cr^{VI} \geq 25$), carbon dioxide (or formic acid) was never detected as a reaction product.

These results were confirmed by HPLC. The chromatograms were obtained on a KNK-500 A chromatograph provided with a 7125

HPLC pump and a 115 Gilson UV–Vis detector. The separation was carried out on an S5 amine resin spherisorb HPLC column using a 73:27 mixture of acetonitrile:0.1 M buffer phosphate (pH 6.4) as eluent and a flow rate of 1.0 mL min^{-1}. For the reactant concentrations used in the kinetic experiments ($[Cr^{VI}] = 8 \times 10^{-4}$ M and [Ald] ≥ 0.02 M), the aldonic acid, and/or the corresponding lactone, of the same number of carbon atoms as the starting sugar was the only reaction product detected by HPLC and it was identified by comparison against authentic samples. Neither alduronic acid nor the lower aldonic acid was observed.

The presence of free radicals was tested for in the reaction of the monosaccharide with Cr^{VI}. In a typical experiment, to a solution of $K_2Cr_2O_7$ (0.0024 mmol) and Ald (0.48 mmol) in 2 mL of 0.5 M $HClO_4$ was added acrylonitrile (0.5 cm^3) at 33 °C. After a few minutes a white precipitate appeared. Control experiments (without $K_2Cr_2O_7$ or reductant present) did not show the formation of a precipitate.

EPR spectroscopy.—The EPR spectra were obtained on a Bruker ESP 300 E spectrometer. The microwave frequency was generated with a Bruker 04 ER (9–10 GHz) apparatus and measured with a Racal-Dana frequency meter. The magnetic field was measured with a Bruker NMR-probe gaussmeter. All of the EPR experiments were carried out at room temperature. A least-squares EPR spectrum-fitting program, e23new, was used to estimate the spectral parameters and relative concentrations of the Cr^V complexes, using Lorentzian line shapes [47,48].

Acknowledgements

The authors thank the National Research Council of Argentina (CONICET), the Third World Academy of Sciences (TWAS), the National University of Rosario, the International Foundation for Sciences (IFS), the National Agency for Sciences Promotion (PICT 0276) and ANTORCHAS Foundation for financial support. They thank Professor S. Brumby and Professor P.A. Lay for providing them with the e23new program.

References

[1] S.A. Katz, H. Salem, *The Biological and Environmental Chemistry of Chromium*, VCH Publishers, New York, 1994, pp. 65–119.
[2] K.D. Sugden, K.E. Wetterhahn, *Chem. Res. Toxicol.*, 10 (1997) 1397–1406.
[3] S. Moghaddas, E. Gelerinter, R.N. Bose, *J. Inorg. Biochem.*, 57 (1995) 135–146.
[4] S.L. Scott, A. Bakac, J.H. Espenson, *J. Am. Chem. Soc.*, 114 (1992) 4205–4213.
[5] M. Costa, *Crit. Rev. Toxicol.*, 27 (1997) 431–442.
[6] H. Lantzsch, T. Gebel, *Mutation Res.*, 389 (1997) 191–197.
[7] M. Ciéslak-Golonka, *Polyhedron*, 15 (1996) 3667–3689.
[8] R.N. Bose, B. Fonkeng, G. Barr-David, R.P. Farrell, R.J. Judd, P.A. Lay, D.F. Sangster, *J. Am. Chem. Soc.*, 118 (1996) 7139–7144.
[9] E.S. Gould, *Coord. Chem. Rev.*, 135/136 (1994) 651–684.
[10] L. Zhang, P.A. Lay, *J. Am. Chem. Soc.*, 118 (1996) 12624–12637.
[11] D.K. Geiger, *Coord. Chem. Rev.*, 164 (1997) 261–288.
[12] K.D. Sugden, K.E. Wetterhahn, *Chem. Res. Toxicol.*, 10 (1997) 1397–1406.
[13] K.E. Wetterhahn Jannette, *J. Am. Chem. Soc.*, 104 (1982) 874–875.
[14] P. O'Brien, J. Barrett, F. Swanson, *Inorg. Chim. Acta*, 108 (1985) L19–L20.
[15] M. Krumpolc, B.G. de Boer, J. Rocek, *J. Am. Chem. Soc.*, 100 (1978) 145.
[16] S.L. Brauer, K.E. Wetterhahn, *J. Am. Chem. Soc.*, 113 (1991) 3001–3007.
[17] D.M.L. Goodgame, P.B. Hayman, D.E. Hathaway, *Polyhedron*, 1 (1982) 497–499.
[18] D.M.L. Goodgame, A.M. Joy, *J. Inorg. Biochem.*, 26 (1986) 219–224.
[19] R. Codd, P. Lay, A. Levina, *Inorg. Chem.*, 36 (1997) 5440–5448.
[20] L.F. Sala, S.R. Signorella, M. Rizzotto, M.I. Frascaroli, F. Gandolfo, *Can. J. Chem.*, 70 (1992) 2046–2052.
[21] S. Signorella, S. García, L. Sala, *Polyhedron*, 11 (1992) 1391–1396.
[22] S.R. Signorella, M.I. Santoro, M.N. Mulero, L.F. Sala, *Can. J. Chem.*, 72 (1994) 398–402.
[23] M. Rizzotto, S. Signorella, M.I. Frascaroli, V. Daier, L.F. Sala, *J. Carbohy. Chem.*, 14 (1995) 45–51.
[24] L.F. Sala, C. Palopoli, S. Signorella, *Polyhedron*, 14 (1995) 1725–1730.
[25] S. Signorella, M. Rizzotto, V. Daier, M.I. Frascaroli, C. Palopoli, D. Martino, A. Bousseksou, L.F. Sala, *J. Chem. Soc., Dalton Trans.*, (1996) 1607–1611.
[26] M. Rizzotto, M.I. Frascaroli, S. Signorella, L.F. Sala, *Polyhedron*, 15 (1996) 1517–1523.
[27] S. Signorella, S. García, L.F. Sala, *Polyhedron*, 16 (1997) 701–706.
[28] C. Palopoli, S. Signorella, L. Sala, *New J. Chem.*, 21 (1997) 343–348.
[29] S. Signorella, M. Santoro, C. Palopoli, C. Brondino, J.M. Salas-Peregrin, M. Quirós, L.F. Sala, *Polyhedron*, 17 (1998) 2739–2749.
[30] V. Daier, S. Signorella, M. Rizzotto, M.I. Frascaroli, C. Palopoli, C. Brondino, J.M. Salas-Peregrin, L.F. Sala, *Can. J. Chem.*, 77 (1999) 1–8.
[31] S.P. Kaiwar, C.P. Rao, *Chem.-Biol. Interact.*, 95 (1995) 89–96.

[32] C.P. Rao, S.P. Kaiwar, *Carbohyd. Res.*, 244 (1993) 15–25.
[33] C.P. Rao, S.P. Kaiwar, *Carbohydr. Res.*, 237 (1992) 195–202.
[34] G.P. Haight, G.M. Jursich, M.T. Kelso, P.J. Merrill, *Inorg. Chem.*, 24 (1985) 2740–2746.
[35] R.G. Wilkins, *The Study of Kinetics and Mechanism of Reactions of Transition Metal Complexes*, Allyn and Bacon, Boston, 1974, pp. 20–23.
[36] M. Krumpolc, J. Rocek, *Inorg. Synth.*, 20 (1980) 63–65.
[37] N.E. Brasch, D.A. Buckingham, A.B. Evans, C.R. Clark, *J. Am. Chem. Soc.*, 118 (1996) 7969–7980.
[38] G. Barr-David, M. Charara, R. Codd, R.P. Farrell, J.A. Irwin, P.A. Lay, R. Bramley, S. Brumby, J.Y. Ji, G.R. Hanson, *J. Chem. Soc. Faraday Trans.*, 91 (1996) 1207–1216.
[39] R.P. Farrell, R.J. Judd, P.A. Lay, R. Bramley, J.Y. Ji, *Inorg. Chem.*, 28 (1989) 3401–3403.
[40] M. Branca, A. Dessí, H. Kozlowski, G. Micera, J. Swiatek, *J. Inorg. Biochem.*, 39 (1990) 217–226.
[41] R. Bramley, J.Y. Ji, R.J. Judd, P.A. Lay, *Inorg. Chem.*, 29 (1990) 3089–3094.
[42] M. Mitewa, R. Bontchev, *Coord. Chem. Rev.*, 61 (1985) 241–272.
[43] S. Signorella, S. García, L. Sala, *J. Chem. Ed.*, in press.
[44] G.R. Buettner, L.W. Oberley, *Biochem. Biophys. Res. Commun.*, 83 (1978) 69–71.
[45] M.E. Trevelyan, D.P. Procter, J.S. Harrison, *Nature*, 166 (1950) 444.
[46] L. Haugh, J.K.N. Jones, W.H. Wadman, *J. Chem. Soc.* (1950) 1702–1706.
[47] S. Brumby, *Appl. Spectrosc.*, 46 (1992) 176–178.
[48] A.L. Beckwith, S. Brumby, *J. Magn. Reson.*, 73 (1987) 252–259.